

## Pre-equilibrium emission *vs.* formation of $^{46}\text{Ti}^*$

M. CICERCHIA<sup>(1)</sup>(<sup>2</sup>)(\*)

<sup>(1)</sup> *INFN Legnaro National Laboratory - Legnaro (PD), Italy*

<sup>(2)</sup> *Department of Physics and Astronomy, University of Padua - Padua, Italy*

received 4 May 2018

**Summary.** — In the NUCL-EX extensive research program on competition between pre-equilibrium and equilibrated source emission, the reactions  $^{16}\text{O}+^{30}\text{Si}$ ,  $^{18}\text{O}+^{28}\text{Si}$  and  $^{19}\text{F}+^{27}\text{Al}$  in the range between 100 and 130 MeV have been measured with the GARFIELD + RCo array at Legnaro National Laboratory. The complete analysis is being performed on an event-by-event basis. The experimental data are compared to the theoretical predictions, where events are generated by numerical codes based on pre-equilibrium and/or statistical models and then filtered through a software replica of the setup. Effects related to the entrance channel and to the colliding ions cluster nature are emphasized through differences between the predictions and the experimental data. After a general introduction on the theoretical basis and on the experimental campaign, some results based on statistical models will be presented in this contribution.

### 1. – Introduction

In the last few decades, the NUCL-EX Collaboration has been engaged in an extensive research program on light excited nuclei decay [1] and on pre-equilibrium emission of light charged particles (LCP) from hot nuclei [2,3] at excitation energies close to LCP emission threshold to study the possible  $\alpha$ -cluster structure in  $\alpha$ -conjugate nuclei. A significant increase in the fast emitted  $\alpha$ -particle yield has been observed: during the 2010s, the analysis of the LCP emission in the  $^{16}\text{O}+^{116}\text{Sn}$  reactions at 8, 12, 16 MeV/u [4-6] brought to the observation of an over-production of  $\alpha$ -particles emitted during the non-equilibrium stage of the nuclear reactions. One quite convincing hypothesis for the  $\alpha$ -particle excess was ascribed to the effects induced by the presence of pre-formed  $\alpha$ -clusters in the  $^{16}\text{O}$  projectile nucleus [7,8]. This excess of counts has been observed in the high energy tail of the experimental  $\alpha$ -distributions with respect to predictions from a hybrid exciton

---

(\*) E-mail: [cicerchia@lnl.infn.it](mailto:cicerchia@lnl.infn.it)

pre-equilibrium model [8, 9], in which the same model parameters were able to reproduce experimental proton distributions. The over-production of the  $\alpha$ -particles could be reproduced when a percentage, close to 50%, of a pre-formation probability in the projectile nucleus was imposed in the simulation code.

To investigate these aspects, in a model independent way, a new experiment was performed to compare results from two reactions induced by projectiles with different probabilities of  $\alpha$ -clusterization: the  $^{16}\text{O}$ , which is a double magic  $\alpha$ -cluster projectile, and the  $^{19}\text{F}$ , which is a non-magic  $\alpha$ -cluster projectile. The two beams at the same beam velocity (close to 16 MeV/u), impinging respectively on  $^{65}\text{Cu}$  and  $^{62}\text{Ni}$  targets, led to the same compound nucleus,  $^{81}\text{Rb}^*$ . Although the analysis is still in progress [2, 10, 11], evidences of an  $\alpha$ -particle fast production excess have been observed for both systems. A slight overproduction has been moreover observed in the  $^{19}\text{F}$  induced reaction with respect to the  $^{16}\text{O}$  one. This could be ascribed to the lower energy of the predicted cluster state of the  $^{19}\text{F}$ .

## 2. – The theoretical issues

The original idea that cluster of nucleons could be preformed in nuclei was introduced by Hafstad and Teller in 1938 [12]. Examining the binding energy per nucleon of the  $\alpha$ -conjugate light nuclei as a function of the mass number, a systematic trend has been found, well described by the liquid drop model as due to a shell structure effect: the  $\alpha$ -conjugate light nuclei are particularly stable and cluster structures are typically observed as excited states close to the decay threshold into clusters. This concept has been summarized, in the late sixties, in the Ikeda diagram [13], which links the energy required to release the cluster constituents to the excitation energy at which the cluster structure prevail in the host nucleus. Afterwards, this concept has been extended to non  $\alpha$ -conjugated nuclei, described in the extended Ikeda diagram [14]; in neutron-rich systems, neutrons may act as valence particles and can be exchanged between the  $\alpha$ -particle cores, in a similar way, electrons are exchanged in atomic molecules. These covalent neutrons stabilize the unstable multi-cluster states, giving rise to nuclear structure which can be described by molecular concepts, well reproduced in model independent approaches like the Fermionic Molecular Dynamics (FMD) [15, 16] or the Antisymmetrized Molecular Dynamics (AMD) with effective N-N forces [17-19]. The study of nuclear states built on clusters bound by valence neutrons in their molecular configurations is a field of large interest, which is being renewed by the availability of exotic beams: clustering is, in fact, predicted to become very important at the drip-line, where weakly bound systems will prevail.

At variance with light nuclei, in which cluster structure might be the preferred structural mode at energy close to particles separation energy [7], this is not established for heavier nuclear systems. An interesting way to investigate the structural properties of medium-mass systems is to study the competition between evaporation and pre-equilibrium particles emission in central collision, as a function of different entrance channel parameters. During the pre-equilibrium emissions, clusters could be engendered by two opposite mechanisms: on one side, the  $\alpha$ -particle is assumed to be preformed inside the nucleus and it could be treated as a single strongly coupled object; on the other side, the coalescence models assume that clusters (not only  $\alpha$ -particle) are formed, in a dynamical way, during the course of the reaction. The dynamical condensation of clusters during nuclear reactions and the preformation of  $\alpha$ -clusters in  $\alpha$ -conjugate nuclei can be studied exploiting stable and exotic beams and searching  $\alpha$ -clustering effects

through the comparison of different experimental combinations of colliding partners and of either excitation or bombarding energies.

Pre-equilibrium LCP and neutrons are fast, forward focused particles emitted during the very early stages of the collision before the attainment of full statistical equilibrium of the compound system. By comparing the yields and the kinematical properties of fast emitted particles with those emitted from a thermalized source, information on the interplay between equilibrium and non-equilibrium processes can be derived as a function of the entrance channel. Even structural properties, like cluster pre-formation probabilities, may be evidenced from the experimental comparison between different reactions leading to the same compound system, reinforced by model predictions. This can be done, for example, by observing and comparing specific exit channels, like those characterized by multiple  $\alpha$ -chains.

### 3. – The experimental details

Non-equilibrium processes, characterizing the early stages of the reaction, play an important role in the dynamics of heavy-ion reactions and contribute to determine the features of the remaining hot thermalized sources. It is known that fast emissions depend both on the entrance channel mass asymmetry and on the beam velocity [20]. The main goal of the experiment, hereinafter described, has been to measure and compare different mass entrance channel reactions with the aim of estimating the pre-equilibrium components; in these medium mass systems, analyzing the competition between the fast emission component with respect to the statistical one and evaluating all possible differences through correlation studies and comparison with model predictions, some information about the influence of structure effects, like  $\alpha$ -clustering, can be derived; differences in LCP angular distributions and LCP emission spectra together with possible anomalies in specific exit channel yields are observed and analyzed.

In this context, a comparative study of four reactions has been designed. The idea is to study these systems in two energy regimes: firstly, at energies close to the onset for the pre-equilibrium emission process, to evaluate its properties in a quite well known framework; then, to carry out a following experiment of the same systems at higher bombarding energies, where the pre-equilibrium part is well assessed and may play a major role.

The first measurement is the object of this paper and involve the four reactions:  $^{16}\text{O}+^{30}\text{Si}$ ,  $^{18}\text{O}+^{28}\text{Si}$  and  $^{19}\text{F}+^{27}\text{Al}$  at 7 MeV/u and  $^{16}\text{O}+^{30}\text{Si}$  at 8 MeV/u.

Through central collisions and with the complete fusion occurring, the four studied cases all lead to the same compound nucleus, the excited  $^{46}\text{Ti}$ , even if with slightly different excitation energies ( $E_{CN}^*(^{16}\text{O}+^{30}\text{Si}$  at 7 MeV/u) = 88.0 MeV;  $E_{CN}^*(^{16}\text{O}+^{30}\text{Si}$  at 8 MeV/u) = 98.4 MeV;  $E_{CN}^*(^{18}\text{O}+^{28}\text{Si}$  at 7 MeV/u) = 98.5 MeV;  $E_{CN}^*(^{19}\text{F}+^{27}\text{Al}$  at 7 MeV/u) = 130.5 MeV); therefore, small differences in their de-excitation chain are expected, except for the cases  $^{16}\text{O}+^{30}\text{Si}$  at 8 MeV/u and  $^{18}\text{O}+^{28}\text{Si}$  at 7 MeV/u, which were chosen to populate the compound nucleus at the same excitation energy. On the other hand, the choice of the same beam energy (7 MeV/u) for three of the four reactions should imply that the non-equilibrium processes are almost the same [20]. Only central collisions will be analyzed in this paper.

A further analysis, dedicated to peripheral collisions, will be performed as a future work, studying the correlations between heavier and lighter emitted clusters, among which  $^{12}\text{C} + \alpha$  for the  $^{16}\text{O}$ ,  $^{14}\text{C} + \alpha$  for the  $^{18}\text{O}$  and  $^{15}\text{N} + \alpha$  in the  $^{19}\text{F}$  case, which can be used to study cluster structure features in the projectile.

**3.1. The experimental array.** – The experiment was performed at the Legnaro National Laboratory (LNL), where the beams  $^{16}\text{O}$  at 111 MeV,  $^{16}\text{O}$  at 128 MeV,  $^{18}\text{O}$  at 126 MeV and  $^{19}\text{F}$  at 133 MeV have been provided by the TANDEM acceleration system and have been used respectively onto the different thin ( $100\ \mu\text{g}/\text{cm}^2$ ) targets:  $^{30}\text{Si}$ ,  $^{28}\text{Si}$  and  $^{27}\text{Al}$ . The employed energies, that were the maximum available with TANDEM alone, were close to the lower thresholds for the pre-equilibrium emission process. The GARFIELD plus Ring Counter (RCo) detector fully equipped with digital electronics [21] has been used to detect LCP, light fragments (LF) and evaporation residues (ER).

The GARFIELD+RCo setup has the capability to measure charge, energy and emission angles of almost all the charged reaction products: particularly, the LCP could be detected in the whole apparatus, while LF and ER have been detected mainly in the forward part (RCo alone). The performances of the apparatus permit the full event reconstruction and the study of many-body correlations; the array has 488 detecting cells with a geometrical coverage of the order of 80% of  $4\pi$ . The two GARFIELD drift chambers cover the  $29^\circ < \theta < 151^\circ$  polar angular range, while the RCo covers the  $5.4^\circ < \theta < 17.0^\circ$ . In the present experiment, due to the high counting rate of elastic scattering, the smallest angles were shielded through an appropriate collimation system; therefore, the Evaporation Residues (ER) have been collected in an angular range  $8.6^\circ < \theta < 17.0^\circ$ , just beyond the grazing angles ( $\theta_{\text{grazing}}(^{16}\text{O}+^{30}\text{Si}$  at 7 MeV/u) =  $10.1^\circ$ ;  $\theta_{\text{grazing}}(^{16}\text{O}+^{30}\text{Si}$  at 8 MeV/u) =  $8.8^\circ$ ;  $\theta_{\text{grazing}}(^{18}\text{O}+^{28}\text{Si}$  at 7 MeV/u) =  $9.0^\circ$ ;  $\theta_{\text{grazing}}(^{19}\text{F}+^{27}\text{Al}$  at 7 MeV/u) =  $8.9^\circ$ ).

The GARFIELD drift chambers are filled with  $\text{CF}_4$  gas at a pressure of 50 mbar. The forward chamber is divided in 24 sectors while the backward chamber in 21 sectors; in each sector 4 gas micro-strips provide the particle energy loss signal,  $\Delta E$ , and 4 CsI(Tl) scintillators, defining four polar angle regions of about  $14^\circ$ , allow to detect the residual energy,  $E$ . Particles identification has been made via  $\Delta E$ - $E$  technique, with an energy resolution of few percent and a threshold of 0.8–1 MeV/u. Furthermore, from CsI(Tl) scintillators LCP masses are also obtained via Fast *vs.* Slow pulse shape analysis technique.

The RCo, suitable to enter in the GARFIELD forward conical opening, is a three-stage annular telescope consisting of an Ionization Chamber (IC), filled with  $\text{CF}_4$  gas and divided in 8 azimuthal sectors; behind each sector, an eight strip  $300\ \mu\text{m}$  thick silicon detector (Si) composes the second stage, followed by the third stage made by 6 CsI(Tl) scintillators. Using the gas section, which was filled at a pressure of 25 mbar in the present experiment, particles and fragments have been identified in charge with energy thresholds of 0.8–1 MeV/u via  $\Delta E$ - $E$  (IC-Si) technique. Moreover, the mass determination for LF (up to  $Z = 12$ ) stopped in the silicon has been obtained, using the pulse shape analysis (PSA) technique in Si, with a quite low threshold ( $\sim 2$ – $4$  MeV/u) [22]. The LCP have been identified via  $\Delta E$ - $E$  (Si-CsI(Tl)) technique and/or through the Fast *vs.* Slow pulse shape analysis of the CsI(Tl) signals technique. Finally, the RCo detector has an angular resolution of  $0.7^\circ$  and an energy resolution of 0.3% for the Silicon strips and 2–3% for the CsI(Tl) scintillators.

Major details on the overall performances are reported in ref. [21].

#### 4. – The data analysis

In this paper, a selected ensemble of events has been chosen, characterizing central collisions; the requested selection has been fulfilled asking for the detection of the ER in the forward direction (RCo) in coincidence with at least one LCP, detected in the whole

apparatus (GARFIELD+RCO). The coincidences with evaporation residues have been set choosing a proper gates in the calibrated charge *vs.* energy spectrum reconstructed from raw data and asking for any coincident particle in the entire apparatus.

Moreover, a further very strict selection on experimental data was performed for the subsequent analysis since an evident O-contamination of the Si (major) and the Al (minor) targets have been observed. Dedicated measurements were performed on the targets themselves with the RBS technique [23], at the LNL AN-2000 accelerator, to define quantitatively the amount of contaminants. A ratio of about 1 was measured for the O with respect to both  $^{30}\text{Si}$  and  $^{28}\text{Si}$  targets, while a ratio of 0.5 was formed in the  $^{27}\text{Al}$  target. Strong effects of such contamination in the  $\alpha$ -particles emission spectra have been observed, which brought to a preliminary wrong interpretation of the experimental data [24]. In order to avoid contaminated data, an almost complete event reconstruction has been requested, which could cut off the unwanted contamination: the considered events are those for which the total detected charge was larger than the 70% ( $Z_{tot} > 16$  for the O+Si cases and  $Z_{tot} > 17$  for the F+Al case) of the expected total charge ( $Z_{projectile} + Z_{target} = 22$ ); a further request was also applied on the relative longitudinal momentum.

**4.1. The statistical simulation code: GEMINI++.** – The analysis has been performed on an event-by-event basis; the experimental observables have been studied and compared with those simulated by the statistical code GEMINI++ [25], which has been used, as a starting point, with standard input parameters and has been coupled with a software replica of the experimental array to take into account the finite size of the detecting device. The GEMINI++ code is based on a complete fusion hypothesis, therefore it can describe the thermalized emission from a CN; on the other hand, it can give information on the expected differences between the four reactions connected to the major part of the cross section, which is related to the de-excitation of a thermalized source (CN). This code is based on the Hauser-Feshbach model, where a quantum description of angular momentum has been joined to the Weisskopf description of evaporation mechanism.

**4.2. Experimental *vs.* simulation comparison.** – The experimental observables of selected events have been compared with the filtered predictions of the theoretical model.

As expected at this bombarding energies, for each studied reaction, the prediction from GEMINI++ accounts for the major part of the cross section both looking at the angular distributions and at the particle energy spectra, demonstrating that complete fusion is the main mechanism occurring between the colliding partners.

The comparison between experimental (black dots) and GEMINI++ (grey triangles) angular distributions for protons (left panels) and for  $\alpha$ -particles (right panels) is displayed in fig. 1 normalized to the area for shape comparison: the proton angular distributions are very similar on the whole angular range; on the contrary, focusing on the  $\alpha$ -particles angular distributions, slight differences are observed at forward angles ( $8.6^\circ < \theta < 17.0^\circ$ ), which may be associated to the small component of  $\alpha$ -particle pre-equilibrium emission (see the following); moreover, another slight difference is present at backward angles ( $115^\circ < \theta < 150^\circ$ ), which has been already pointed out in our previous work [1]. To give an explanation of this excess further analysis is needed, taking into account angular momentum or possible deformation effects. A similar behaviour is confirmed by the proton and  $\alpha$ -particle energy distributions, normalized to the experimental maximum, in the laboratory frame and in the whole detection angular range: all the proton spectra are quite well accounted for by a statistical description, while some deviations appear in the case of  $\alpha$ -particles.

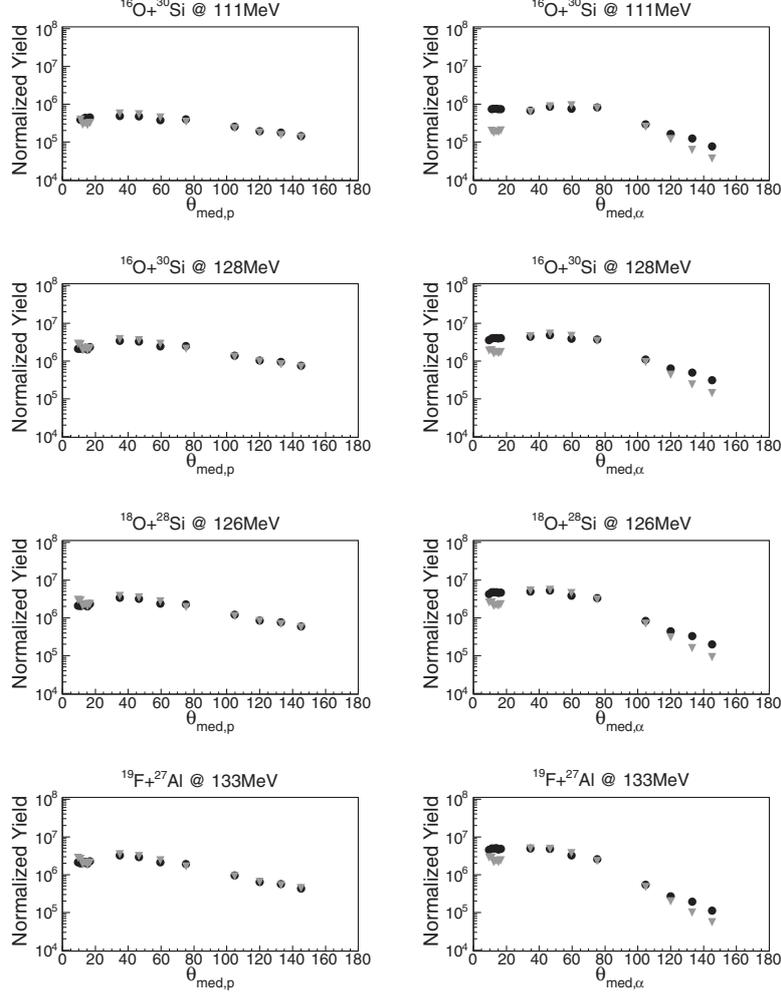


Fig. 1. – Comparison between experimental (black dots) and GEMINI++ simulated (grey triangles) angular distribution of proton (left panels) and  $\alpha$ -particles (right panels) in coincidence with ER from the four reaction, from the top to bottom,  $^{16}\text{O}+^{30}\text{Si}$  at 7 MeV/u,  $^{16}\text{O}+^{30}\text{Si}$  at 8 MeV/u,  $^{18}\text{O}+^{28}\text{Si}$  at 7 MeV/u and  $^{19}\text{F}+^{27}\text{Al}$  at 7 MeV/u. Experimental and simulated distributions are normalized to the area.

These differences seem to depend on the particular entrance channel; in fig. 2, the proton (left panels) and  $\alpha$ -particles (right panels) energy spectra for the four reactions are shown for the forward angle  $10.3^\circ < \theta < 11.7^\circ$ , where GEMINI++ well reproduce the proton spectra, while the disagreement in  $\alpha$ -particle spectra are evident. In particular, the larger difference can be observed in the  $^{16}\text{O}$  induced reaction at the higher bombarding energy. This is, somehow, expected due to the slight higher beam velocity involved (8 MeV/u). Moreover, smaller and similar deviations are also pointed out in the case of  $^{18}\text{O}+^{28}\text{Si}$ ,  $^{19}\text{F}+^{27}\text{Al}$  and  $^{16}\text{O}+^{30}\text{Si}$  at 7 MeV/u. A quantitative analysis on the observed differences is in progress to give a clearer interpretation of the results, through the comparison with a Pre-equilibrium Hybrid Model [8].

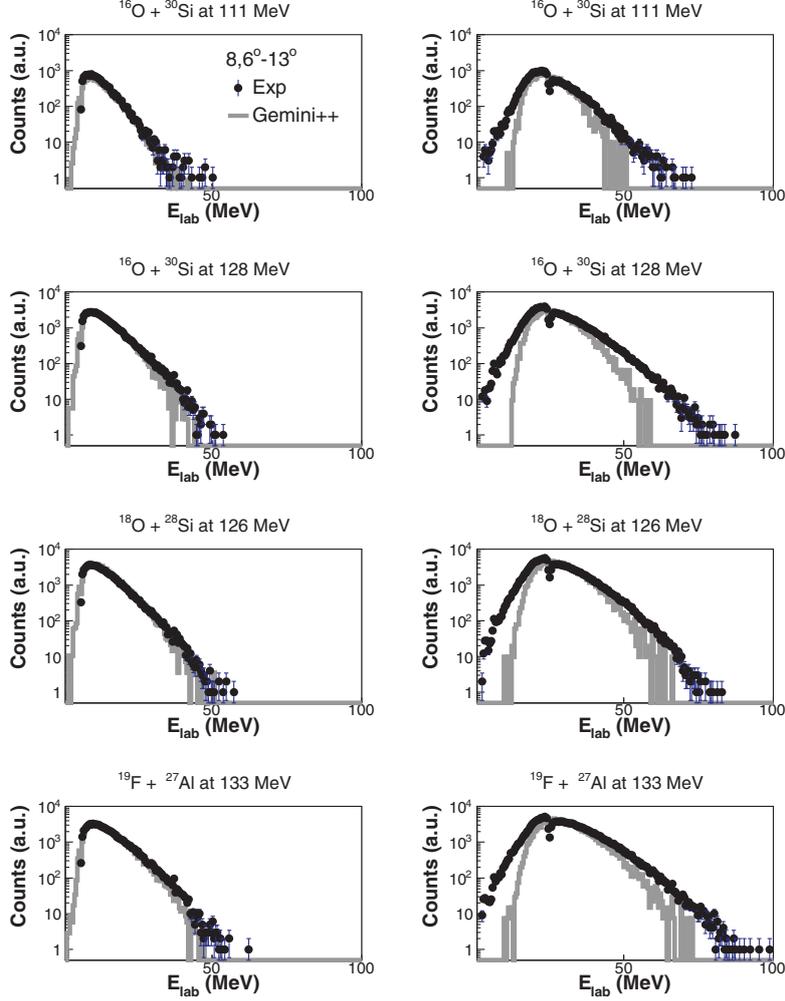


Fig. 2. – Comparison between experimental (black dots) and GEMINI++ simulated (grey triangles) forward ( $10.3^\circ < \theta < 11.7^\circ$ ) spectra of proton (left panels) and  $\alpha$ -particles (right panels) in coincidence with ER from the four reaction, from the top to bottom,  $^{16}\text{O} + ^{30}\text{Si}$  at 7 MeV/u,  $^{16}\text{O} + ^{30}\text{Si}$  at 8 MeV/u,  $^{18}\text{O} + ^{28}\text{Si}$  at 7 MeV/u and  $^{19}\text{F} + ^{27}\text{Al}$  at 7 MeV/u. All spectra are normalized to experimental maximum.

Looking at more exclusive observables, *i.e.* the multiplicity distributions, further interesting differences between the four studied reactions can be highlighted. In fig. 3 one can see that the multiplicities of proton (left panels) and  $\alpha$ -particles (right panels), which have been normalized to the number of selected ER, are overestimated by the code for low multiplicity ( $M_{p,\alpha} \leq 3$ ), in agreement with the literature systematics. On the contrary, they appear more or less underestimated for  $M_{p,\alpha} > 3$  depending on the different studied systems. Indeed, this may indicate, like it was shown in our previous work [1], that specific branching ratios of selected channels and reconstructed  $Q$ -values distributions may lead to quite different results, especially when multiple  $\alpha$ -particles are involved in the decay.

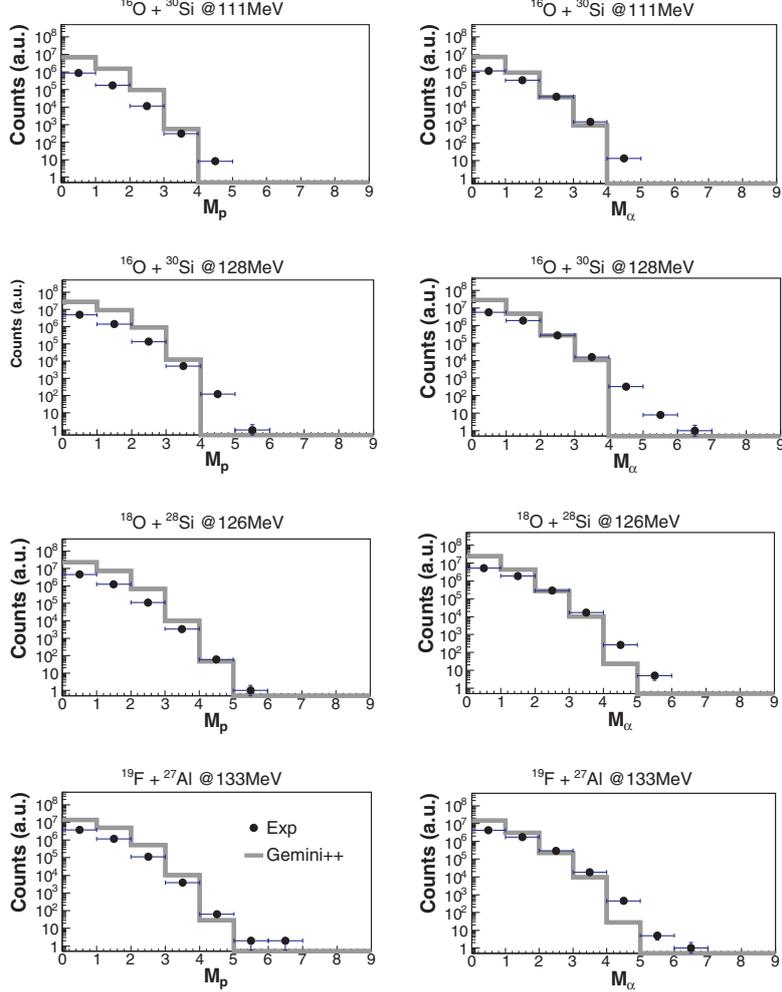


Fig. 3. – Comparison between experimental (black dots) and GEMINI++ simulated (grey triangles) multiplicity distributions for proton (left panels) and  $\alpha$ -particles (right panels) in coincidence with ER from the four reaction, from the top to bottom,  $^{16}\text{O} + ^{30}\text{Si}$  at 7 MeV/u,  $^{16}\text{O} + ^{30}\text{Si}$  at 8 MeV/u,  $^{18}\text{O} + ^{28}\text{Si}$  at 7 MeV/u and  $^{19}\text{F} + ^{27}\text{Al}$  at 7 MeV/u. All distributions are normalized to the number of ER.

Since the onset of pre-equilibrium emission has been observed, the differences between the four studied reactions cannot be reproduced by using simply the statistical code GEMINI++, but it is necessary to compare data to model simulations able to take into account even the dynamical part of the reactions, like the Moscow Pre-equilibrium Model by Fotina [8] or the AMD code by Ono [17]. These further studies and some cross-check, which are undergoing, are needed before addressing any complete conclusion. However, the differences observed in this preliminar analysis indicate that interesting and new information can be obtained studying in detail these systems: in particular, the observed difference in multiple  $\alpha$ -decay channel may be related to different structural effects of the colliding partners.

## 5. – Conclusions and perspectives

In order to probe the competition between thermal and fast emission processes and the possible  $\alpha$ -clustering effects on dynamics, the comparative study of the four reactions,  $^{16}\text{O}+^{30}\text{Si}$  at 8 MeV/u,  $^{16}\text{O}+^{30}\text{Si}$ ,  $^{18}\text{O}+^{28}\text{Si}$  and  $^{19}\text{F}+^{27}\text{Al}$  at 7 MeV/u, has been carried out at LNL. In this paper, the attention has been focused on the comparison between experimental observables with those simulated by the statistical code GEMINI++. Differences between the experimental and the predicted observables put into evidence effects related to the entrance channels and to a small contribution from fast emission. Studying the decay of  $^{46}\text{Ti}^*$ , formed in the case of complete fusion, the GEMINI++ simulations reasonably reproduce most global variables for all the reactions; nevertheless, the slight differences observed are crucial for analyzing the interplay between the two different reaction mechanisms. In particular, the overproduction of  $\alpha$ -particles of forward angles represents a signature of the onset of fast emission. To understand if the pre-equilibrium process is well accounted for by theory, a quantitative analysis is needed. A comparison to predictions by the Moscow Pre-equilibrium Model [8], based on the Hybrid model [9], which takes into account a pre-equilibrium stage before a second thermalized emission stage, is undergoing. Moreover, simulations based on modern dynamical models, like AMD [17], which can take into account not only the dynamics of the reaction, but also the possible influence of the structural effects in the following path of the reaction, are also under study and will be used in forthcoming more exclusive analysis [26]. Indeed, the differences in specific multiplicity channels have been noticed with consequences on the branching ratios and  $Q$ -value distributions. Lastly, to complete this experimental campaign, new measurements of the same systems ( $^{16}\text{O}+^{30}\text{Si}$ ,  $^{18}\text{O}+^{28}\text{Si}$  and  $^{19}\text{F}+^{27}\text{Al}$ ) need to be carried out at higher energies (12–16 AMeV), where larger pre-equilibrium yields and higher excitation energies are foreseen: in fact, the analysis of correlations between LCP particles, especially in long  $\alpha$ -decay chains ( $M_\alpha \geq 3$ ) events, is necessary to constraint the dynamics and to draw conclusions on the differences among the studied systems and on their possible link to structural effects of the colliding partners.

\* \* \*

I would like to acknowledge the NUCL-EX Collaboration for giving me the opportunity to analyze the data object of this article and for lending me the code which was used to perform the simulations, in particular the LNL-Pd group for helping me in the interpretation of the results. I express my gratitude to F. Gramegna, my PhD supervisor from LNL, for the help during the writing of this paper and for the valuable discussions. Special thanks go to the SIF Scientific Committee for reporting my presentation as the best of the first section (*Fisica nucleare e subnucleare*) and, then, for giving me the opportunity to write this article.

## REFERENCES

- [1] MORELLI L. *et al.*, *J. Phys. G*, **41** (2014) 075107; MORELLI L. *et al.*, *J. Phys. G*, **41** (2014) 075108.
- [2] FABRIS D. *et al.*, *PoS, X LANSPA* (2013) 061.
- [3] FOTINA O. *et al.*, *EPJ Web of Conferences*, **66** (2014) 03028.
- [4] FOTINA O. *et al.*, *Int. J. Mod. Phys. E*, **19** (2010) 1134.
- [5] KRAVCHUK V. L. *et al.*, *EPJ Web of Conferences*, **3** (2010) 10006.
- [6] CORSI A. *et al.*, *Phys. Lett. B*, **679** (2009) 197.

- [7] FREER M. *et al.*, *Rep. Prog. Phys.*, **70** (2007) 2149.
- [8] FOTINA O. *et al.*, *Phys. At. Nucl.*, **73** (2010) 1317.
- [9] GRIFFIN J. J., *Phys. Rev. Lett.*, **17** (1966) 478.
- [10] GRAMEGNA F. *et al.*, *J.Phys. Conf. Series*, **580** (2015) 012011.
- [11] FABRIS D. *et al.*, *EPJ Web of Conferences*, **163** (2017) 00016; FABRIS D. *et al.*, in preparation.
- [12] HAFSTAD L. R. and TELLER E., *Phys. Rev.*, **54** (1938) 681.
- [13] IKEDA K., TAGIKAWA N. and HORIUCHI H., *Prog. Theor. Phys. Suppl.*, **1968** (464).
- [14] VON OERTZEN W., FREER M. and KANADA-ENYO Y., *Phys. Rep.*, **432** (2006) 43.
- [15] FELDMER H. *et al.*, *Nucl. Phys. A*, **586** (1995) 493.
- [16] NEFF T., FELDMER H. and ROTH R., *Nucl. Phys. A*, **752** (2005) 94.
- [17] ONO A., *EPJ Web of Conferences*, **31** (2012) 00023.
- [18] HORIUCHI H. and KANADA-ENYO Y., *Nucl. Phys. A*, **612** (1997) 394c.
- [19] KANADA-ENYO Y. and HORIUCHI H., *Prog. Theor. Phys. Suppl.*, **142** (2001) 206.
- [20] HODGSON P. E. and BÉTÁK E., *Phys. Rep.*, **374** (2003) 1.
- [21] BRUNO M. *et al.*, *Eur. Phys. J. A*, **49** (2013) 128 and references therein; GRAMEGNA F. *et al.*, *Nucl. Instrum. Methods A*, **389** (1997) 474.
- [22] LE NEINDRE *et al.*, *Nucl. Instrum. Methods*, **205** (2013) 145.
- [23] CHU W. K., MAYER J. W. and NICOLET M. A., *Backscattering Spectrometry* (Academic Press, New York) 1978; FELDMAN L. C. and MAYER J. W., *Fundamentals of Surface and Thin Film Analysis* (Elsevier Science Publishing Co.) 1986.
- [24] GRAMEGNA F. *et al.*, *EPJ Web of Conferences*, **163** (2017) 00020.
- [25] CHARITY R. J., *Phys. Rev. C*, **82** (2010) 014610.
- [26] FABRIS D. *et al.*, *EPJ Web of Conferences*, **163** (2017) 00016.